Supporting Information

Wang *et al.* 10.1073/pnas.0710092105

SI Text

AUC Analysis. The binary mixture of SA and SD (Fig. S3*B* and Table S1) produced a boundary in which the 2 species could not be distinguished, owing to the similarity of their sedimentation coefficients (for the mixture of SA and SD $s = 2.1 \pm 0.01$S), but with a very small amount of a faster-moving species apparent that was not visible in the pure systems ($s = 6.2 \pm 0.3$S). The binary mixture of SD and GNBP1 displayed 4 distinguishable species, with sedimentation coefficients of 2.0 ± 0.01S, 3.2 ± 0.01S, 4.0 ± 0.3S, and 5.6 ± 0.7S (Fig. S3*C* and Table S1). We are confident, on the basis of comparison with the pure systems, in identifying the species at 2S with PGRP-SD and that at 3.2S with GNBP1. The species at 5.6S tallies with that at a similar value seen in pure GNBP1 (5.5S), and we therefore believe that the species at 4.0S is a complex between GNBP1 and PGRP-SD. The binary mixture of PGRP-SA and GNBP1 again displayed 4 distinguishable species, with sedimentation coefficients of 2.0 ± 0.01S, 3.5 ± 0.01S, 4.5 ± 0.2S, and 6.7 ± 0.02S (Fig. S3*D* and Table S1). The first three are easily identifiable with reference to the pure systems and the mixture of PGRP-SD and GNBP1 as follows: PGRP-SA (2S), GNBP1 monomer (3.5S), and the complex of PGRP-SA and GNBP1 (4.5S). The species at 6.7S might be a complex of GNBP1 molecules, or some other kind of aggregate.

The ternary mixture of PGRP-SA, SD, and GNBP1 gave up to 8 distinguishable peaks, as listed in Table S1. An inset to Fig. S3*E* shows these species, but the main figure focuses in on the region up to 10S. Here, the 3 apparent species can be identified as PGRP-SA and PGRP-SD in the peak at 2S. The peak at 5.8S was broad and likely to be contributed by both PGRP-SA-GNBP1 and PGRP-SD-GNBP1. The peak at 7.1S is likely to be the ternary complex. The breadth of the distributions observed may arise from the exchange of binding partners over the time course of the experiment, suggesting a rapid exchange of interactions at equilibrium in this mixture.

Addition of highly purified tetrameric muropeptide from *S. aureus* at a concentration of 10 μM changed the behavior of binary and ternary mixtures of the proteins. The combination of PGRP-SD and GNBP1 with muropeptide displayed 5 identifiable species, four of which present a similar profile to the mixture without peptide (Fig. S3*F* and Table S1). The peak at 1.9S is identifiable with PGRP-SD, and that at 3.6S with GNBP1. We suggest the peak at 1.1S reflects the sedimentation of the peptide or an aggregate of it, and that at 2.6S as GNBP1. This value was significantly lower than those measured for GNBP1 alone and in other mixtures; we nevertheless ascribed this peak to it because of visual comparison of the profiles with and without peptide (as accentuated by the lines linking peaks in Fig. S3) and suspect that the low value determined here may be a function of a lack of resolution and difficulty in deconvoluting multiple Gaussian distributions uniquely. The superposition of the c(s,M) arrays for GNBP1 and PGRP-SD with and without muropeptide (Fig. S5*D*) strongly argue to equivalence between the peaks but the patterning of the contours.

Addition of the peptide produced a greater change on the profile of GNBP1 and PGRP-SA than it did on GNBP1 and PGRP-SD. Overall, there was a marked tightening of the Gaussian distributions in the mixture of PGRP-SA, GNBP1, and muropeptide, in which 7 species were thereby identifiable (Fig. S3*G* and Table S1). As usual, PGRP-SA and GNBP1 are individually apparent, as well as peaks derived from the peptide alone and a new species that we take to be the PGRP-SA-peptide complex (1.3 and 2.9S). In addition, the peak at 4.8S derives we conclude from the mixture of PGRSA, GNBP1, and peptide, as also visualized in the mixture without peptide (at 4.5S). These correlate with results from native gels described (1). The presence of the peptide did not seem to have markedly increased the amount of GNBP1-SA observed, but it has increased the resolution of the profile (lifetime of the complexes) owing to better definition between the different complexes in the mixture (i.e., a lower k_{off}). In conclusion, addition of the highly purified tetrameric muropeptide from *S. aureus* dramatically changed the g(s) distributions and the subsequent weight identities of the GNBP1/PGRP-SA/PGRP-SD mixture to a far clearer picture.

In the contour plots the distribution of c(s,M) for GNBP1 indicated a molecular mass in the region of 60 kDa and that the higher sedimentation coefficient (≈5.7S) species noted in the analysis of g(s) had a molecular weight of approximately 120 kDa, consistent with its identification as a dimer. For both PGRP-SA and PGRP-SD individually and for the binary mixture of the two, the c(s,M) distribution indicated that the sedimentation coefficient and the expected weight match ($M = 20$ kDa). The plots with mixtures of GNBP1 and SA or SD were consistent with the formation of the complexes noted for the g(s) analysis, with species appearing with the correct weight in each. Accordingly, there was an extension in the c(s,M) distribution above the range occupied by GNBP1 alone to a higher s and M, reaching 80 kDa in both cases. In the presence of the muropeptide this redistribution was strengthened. The most dramatic effects of the muropeptide were, however, found in the ternary mixture, where the occupancy of the ternary complex and its resolution seemed significantly enhanced by the presence of the peptide. Our results are illustrated in Fig. S4. Fig. S5 illustrates the direct superposition of the c(s,M) components of the c(s,M) plots in Fig. S4. This allows us to make more clearly the point that the patterns of sedimenting species are consistent between pure samples and their mixtures, and, most importantly, that the inclusion of the muropeptide clearly allows the formation of novel complexes and tightens (i.e., increases the presence of) others.

In Fig. S5*A*, we show the data for SA and SD alone and when combined. As in Fig. S3*A* and *B*, the predominant species is at 2S and PGRP-SA and PGRP-SD show a similar pattern of c(s,M), maintained when mixed.

In Fig. S5*B*, we show the data for GNBP1 alone and when mixed with PGRP-SA and SD. As previously observed, GNBP1 shows evidence of a species which s and M indicate to be monomeric (60 kDa) of a dimer (120 kDa). This sensitive c(s,M) analysis also indicates the possible existence of a tetramer (240 kDa). Addition of PGRP-SA and SD give patterns of c(s,M) that are quite distinctive: the lower M_w peak shifts upward slightly, the higher ones weaken, and the individual peaks for PGRP-SA and SD are less prominent than in the pure mixtures of the two. That is, PGRP-SA and SD have both bound to GNBP1, resulting in an upward shift in the GNBP1 monomer peak, lessening of the GNBP1 oligomer peaks (due to sequestration of GNBP1 into complexes), and lowering of PGRP-SA and SD peaks.

In Fig. S5*C*, we show the data for GNBP1 mixed with PGRP-SA, and for the same mixture with the muropeptide added. For these two experiments rather similar species distributions are seen, which is in strong support of our conclusion that related species can be identified in the two mixtures, as previously with reference to Fig. S3*D* and *G*. However, as before, it is clear there is a strengthening of the higher-weight complexes

(they have higher occupancy in the 2-dimensional c(*s*,*M*) plots) in the presence of the muropeptide, and there is a suggestion (due to a downward shift in apparent sedimentation coefficient) that the conformation of the GNBP1-PGRP-SA-peptide complex is more compact than that of GNBP1-PGRP-SA lacking muropeptide.

The effects of the muropeptide on the mixture of GNBP1 and PGRP-SD (Fig. S5*D*) are very similar to those on GNBP1 with PGRP-SA, including a smaller downward shift in *s*. The increased occupancy of complexes is obvious in the presence of the peptide. Furthermore, as in comparison between Fig. S3*C* and Fig. S3*F*, a related pattern is clearly present in the mixture with and without muropeptide (as commented above for Fig. S5*C*).

As before, the effects of the muropeptide are most marked for the ternary complex of GNBP1, PGRP-SA, and SD, where its presence brings about the appearance of a strong complex peak at 8S and 100 kDa, the expected weight of a GNBP1-SA-SD oligomer (Fig. 4*E*).

Differences in PG Structure Between *Ml*, *Sa*, and *Ss*. In Gram-positive bacteria, PG constitutes a significant fraction of the bacterial surface and shows considerable level of heterogeneity. It is directly exposed to the surrounding media together with any polysaccharides or proteins that may be attached to it. In the present report we have used purified PG from three different bacteria to study the recognition process needed to induce an innate immune response in *Drosophila*. These bacteria have a different PG composition and different ability to produce disease in the host.

Micrococcus luteus is a nonpathogenic, Gram-positive bacterium described as carrying a unique PG type A11.pep (2). In this PG, a peptide subunit is involved in the cross-linkage of 2 other peptide subunits that are connected to the glycan chains. The peptide subunit is composed by the sequence NH_2-L-Ala-D-Glu(Gly)-L-Lys-D-Ala-D-Ala-COOH. The glycine residue is linked to the α-carboxyl group of the glutamic acid, and the D-alanine at the carboxyl terminus may be removed by endogenous bacterial DD-carboxypeptidases. However, a high number of N-acetylmuramic acid residues in the glycan chains are not linked to peptide subunits.

The genus *Staphylococcus* includes Gram-positive bacteria that are frequent colonizers of the human skin and mucous membranes. It can be divided into two subgroups based on the ability of a species to produce the blood-clotting enzyme coagulase. The coagulase-negative staphylococci, such as *Staphylococcus saprophyticus* among others, are considered to be opportunist pathogens. However, *Staphylococcus aureus* is the only coagulase-positive species of this genus and is a well known human pathogen.

Both species, *S. saprophyticus* and *S. aureus*, produce similar PGs of type A11.3 and A11.2 respectively. In both PGs the peptide subunit is composed by the sequence NH_2-L-Ala-D-Glu(NH_2)-L-Lys-D-Ala-D-Ala. However, in *S. aureus* the α-carboxyl group of the D-Glu is amidated, and the ε aminogroup of the lysine residue is linked to a pentaglycine bridge (type A11.2) as opposed to a pentaglycine bridge in which one or two of these glycines may be substituted by serines (type A11.3 in *S. saprophyticus*).

In conclusion, the nature of PG cross-linking (*Sa* vs. *Ss*) and extent of this (*Sa* and *Ss* vs. *Ml*) denote the differences between these PGs.

1. Wang L, Weber AN, Atilano ML, Filipe SR, Gay NJ, *et al.* (2006) Sensing of Gram-positive bacteria in *Drosophila*: GNBP1 is needed to process and present peptidoglycan to PGRP-SA. *EMBO J* 25:5005–5014.
2. Scheifer KH, Kandler O (1972) Peptidoglycan types of bacterial cell walls and their taxonomic implications. *Bacteriol Rev* 36:407–477.
3. Filipe SR, Tomasz A, Ligoxygakis P (2005) Requirements of peptidoglycan structure that allow detection by the *Drosophila* Toll pathway. *EMBO Rep* 6:327–333.

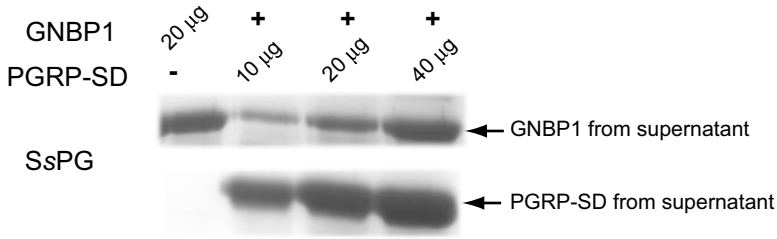

Fig. S1. Binding assay was performed as described in Fig. 2 and Materials and Methods. After binding to *Ss* PG supernatant was retained in this experiment, and proteins were acetone-precipitated. From one point on, with increasing amounts of PGRP-SD, more GNBP1 could be removed from binding to PG.

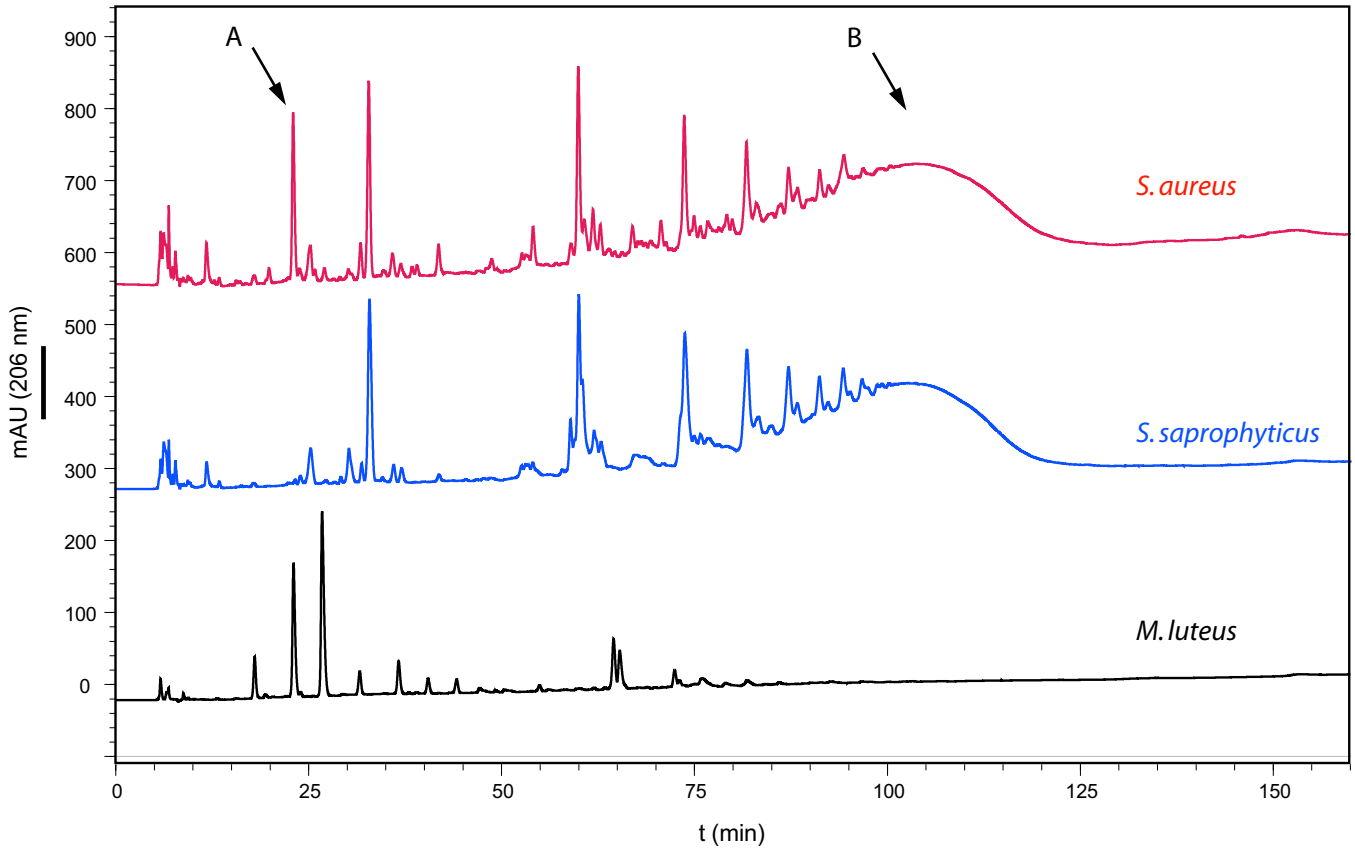

Fig. S2. Differences between PGs from *M. luteus*, *S. saprophyticous*, and *S. aureus*. HPLC analysis of muropeptide composition of PG purified from *S. aureus* COL strain (red), *S. saprophyticus* ATCC15305 strain (blue), *M. luteus* DSM20030 strain (black). Purified PG was digested with mutanolysin and the released muropeptides analyzed by HPLC as described (2, 3). The differences observed when comparing *S. aureus* and *S. saprophyticus* are labeled with arrows as (*A*) the presence in *S. aureus* of a monomeric muropeptide with no pentaglycine bridge and (*B*) a different curve shape that corresponds to a different level of cross-linking. The profile observed with *M. luteus* PG reflected the dissimilar muropeptide make-up in terms of amino acid composition and cross-linking type.

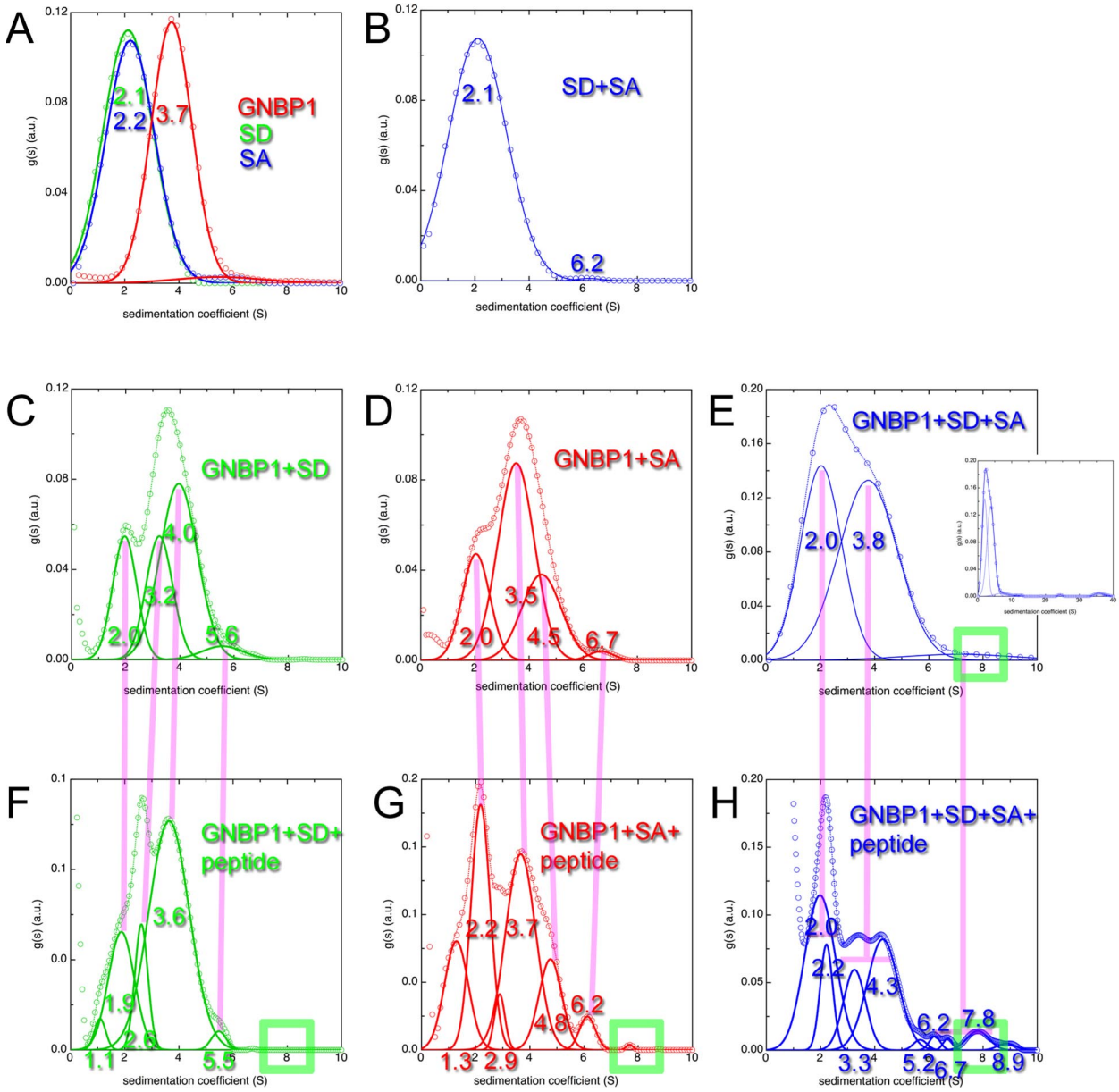

Fig. S3. Ternary complex and heterodimeric formations in the presence of a highly purified muropeptide. AUC experiments were performed to determine the change in receptor associations in the presence of a microbial ligand. (*A*) Sedimentation coefficient profiles (g(s)) for PGRP-SA (blue symbols and line), PGRP-SD (green symbols and line), and GNBP1 (red symbols and lines). (*B–H*) As in *A* for the species indicated. In each case the data (symbols), the global fit (dotted line), and the component Gaussian distributions that together compose it (solid lines) are shown. The pink transparent lines link the same species identified in different mixtures, and the green transparent boxes mark the region in which a significant amount of complex was observed appearing in the ternary mix when a tetrameric muropeptide from *S. aureus* was added (see *SI Text* for details).

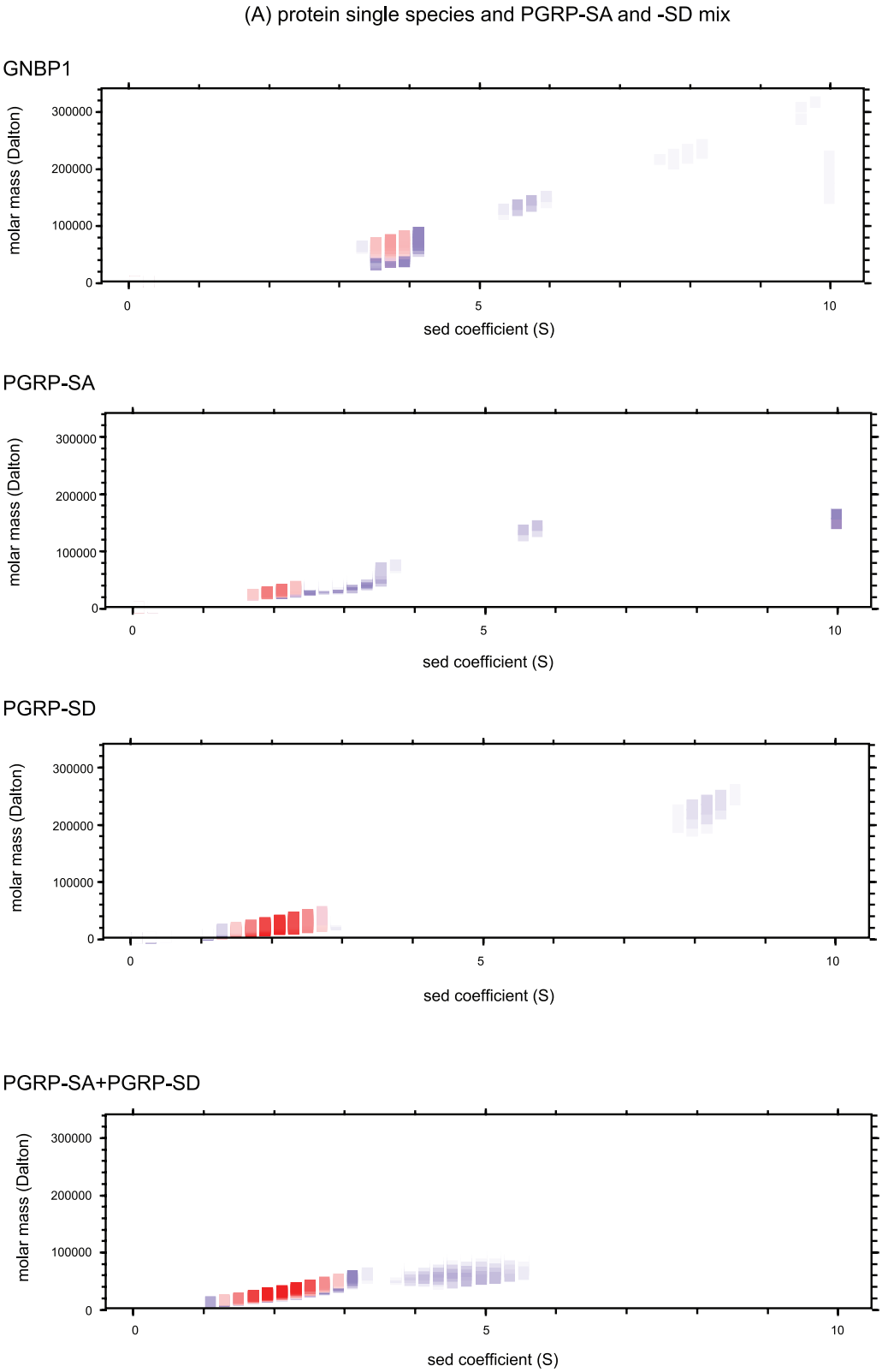

Fig. S4. Further analysis of AUC data. Plots are shown of c(*s*,*M*), where the vertical axis is sedimentation coefficient, *s*, and the vertical the molar mass or weight, *M*. These plots allow correlation of *s* to *M* by allowance for the frictional effects of shape on *s*. Crucially they show the marked effect of the *S. aureus* tetrameric muropeptide on the associational properties of this system. The color scale (blue to red) represents increasing intensity within these two-dimensional plots (i.e., peak height).

(B) GNBP1 with PGRP-SA and -SD with/without the presence of muropeptide

GNBP1+PGRP-SA

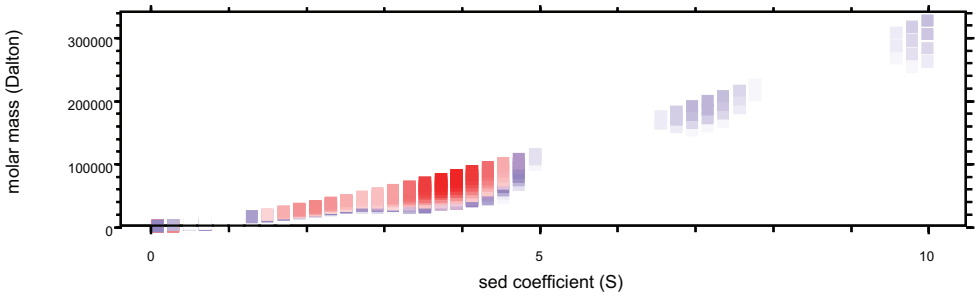

GNBP1+PGRP-SA+muropeptide

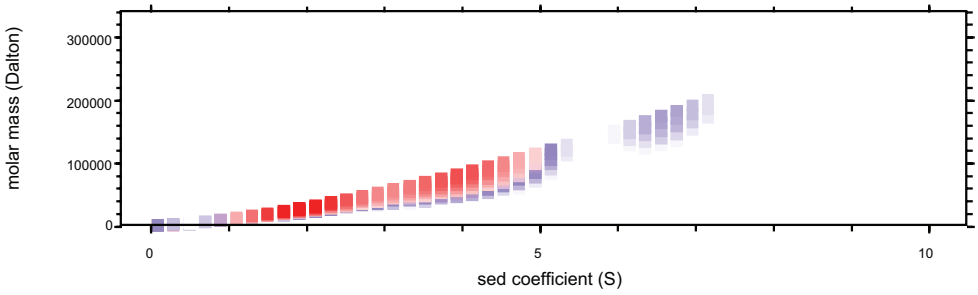

GNBP1+PGRP-SD

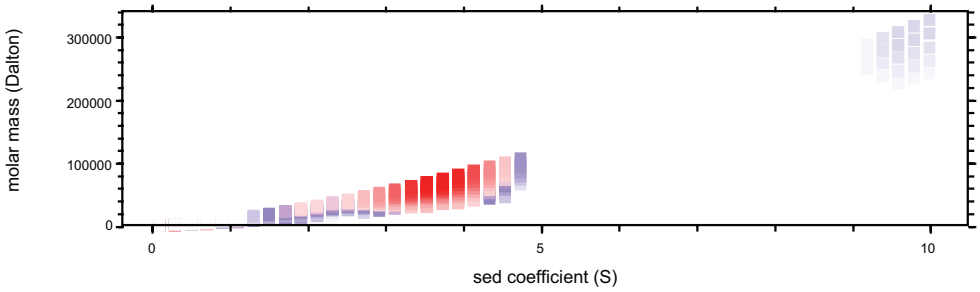

GNBP1+PGRP-SD+muropeptide

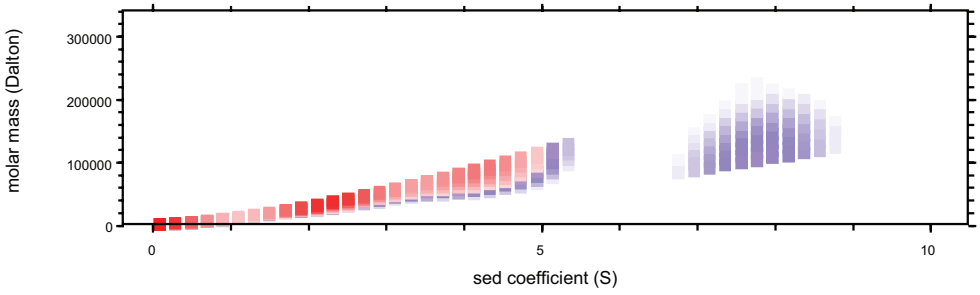

Fig. S4. (continued)

(C) Tripartite protein interaction with/without the presence of muropeptide

GNBP1+PGRP-SA+PGRP-SD

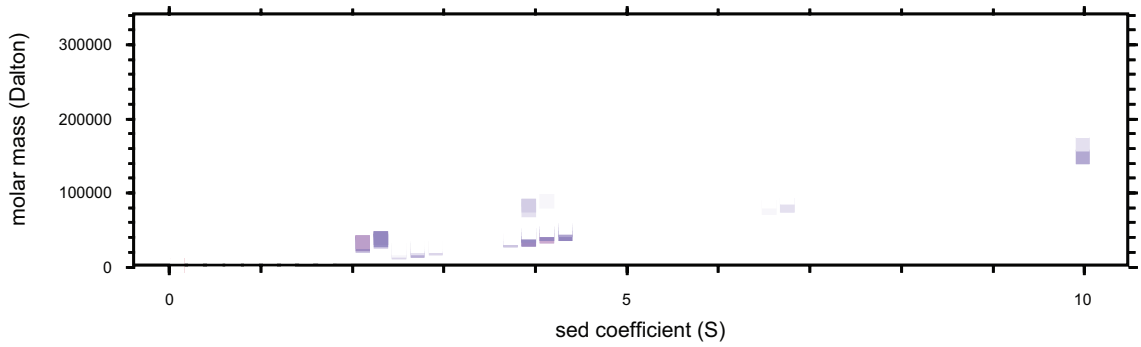

GNBP1+PGRP-SA+PGRP-SD+muropeptide

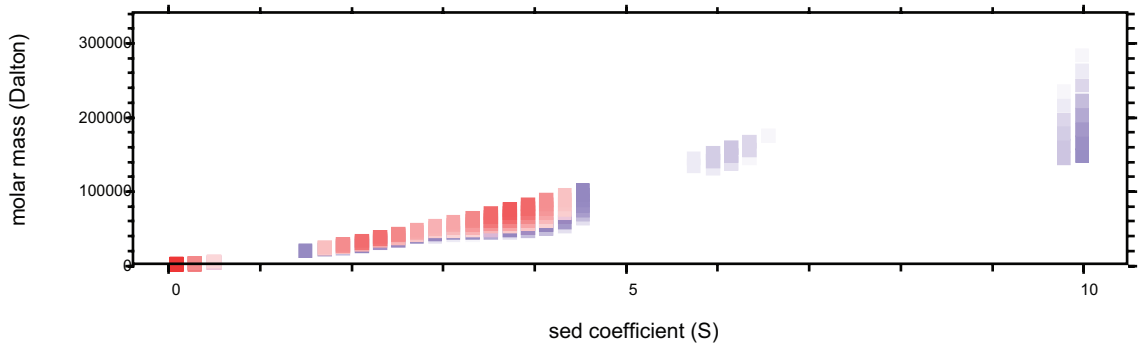

Fig. S4 (continued).

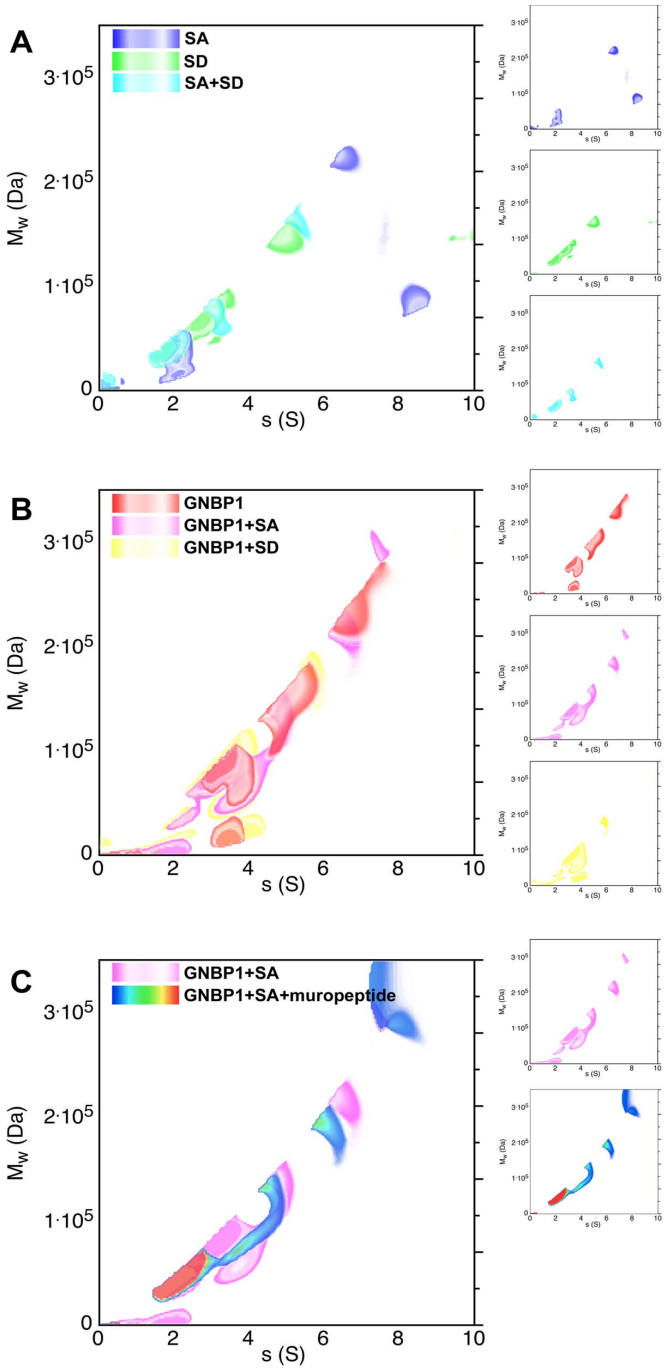

Fig. S5. Higher resolution of AUC temperature plots. Two-dimensional plots of c(*s*.*M*) are shown. (*A*) For SA (blue contours), SD (green), and a mixture (cyan). To the right the individual plots are shown. (*B*) As *A*, for GNBP1 (red contours), GNBP1+SA (magenta), and GNBP1+SD (yellow). (*C*) As *A*, for GNBP1+SA (magenta contours) and the same with muropeptide (multicolour contours). (*D*) As *C*, for GNBP1+SD (yellow contours) and the same with muropeptide (multicolour contours). (*E*) As *C*, for GNBP1+SA+SD (orange contours) and the same with muropeptide (multicolour contours). These plots are all essentially higher-resolution depictions of data already presented as the temperature plots in Fig. S4.

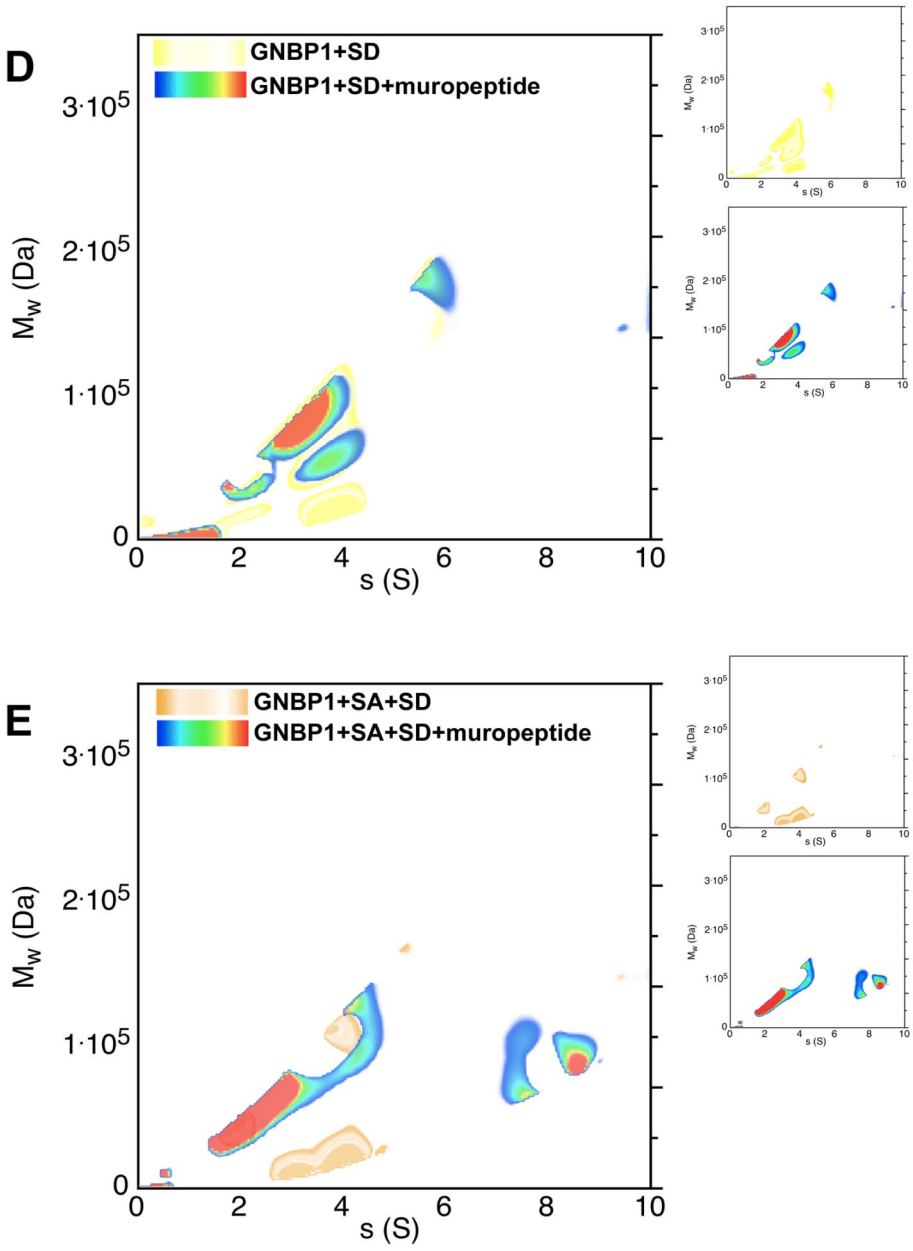

Fig. S5 (continued).

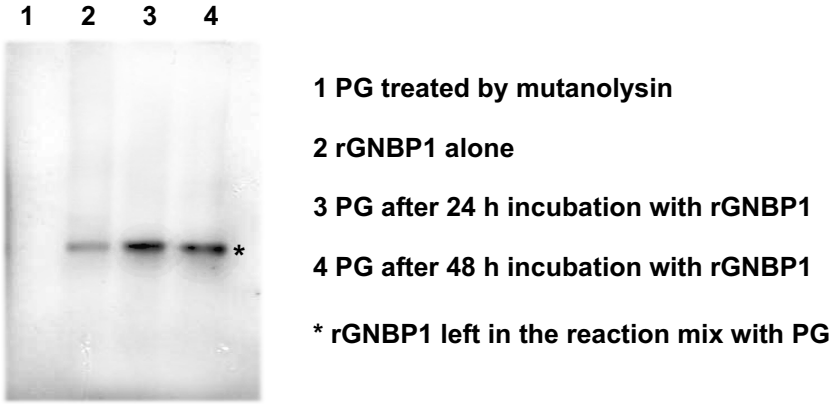

Fig. S6. PG controls in native gel analysis. PG alone used in the native gel analysis of Fig. 4 was analyzed under the same electrophoresis conditions on 4–12% native Tris-glycine gel as described in Fig. 4 main text and the relevant section of Material and Methods. From left to right: lane 1, mutanolysin-treated PG; lane 2, rGNBP1 alone; lanes 3 and 4, PG after 24 h and 48 h incubation with rGNBP1, respectively. No protein complexes or PG degradation products were observed. Gels were stained with Coomassie blue reagent using SimplyBlue Invitrogen.

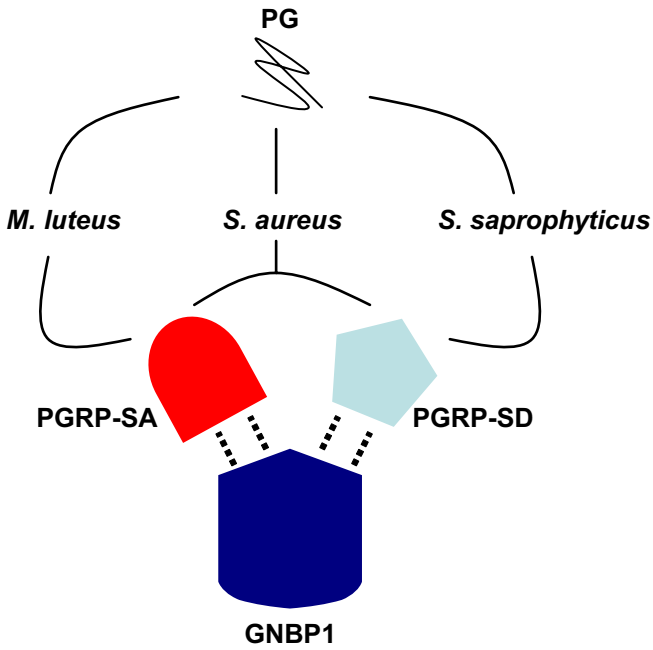

Fig. S7. Schematic representation of a model for host receptor formation during gram-positive bacterial sensing in *Drosophila*. The ternary complex (central branch) or the various combinations of heterodimers may be formed depending on the type of PG sensed. The heterodimers will be either PGRP-SD/GNBP1 for sensing of *S. saprophyticus* PG or PGRP-SA/GNBP1 for sensing of *M. luteus* PG. The ternary complex will form when sensing *S. aureus* PG. Refer to Discussion for details.

Table S1. Identification of protein species in AUC analysis.

SA	SD	GNBP1	SA-SD	SD-GNBP1	Ratio	SA-GNBP1	Ratio	SA-SD-GNBP1	SD-GNBP1-peptide	Ratio	SA-GNBP1-peptide	Ratio	SA-SD-GNBP1-peptide	Ratio	Posited identity
									1.1±0.01	**1**	1.3±0.01	**10**			
2.2±0.01	2.1±0.01		2.1±0.01	2.0±0.01	**25**	2.0±0.01	**10**	2.0±0.02	1.9±0.01	**8**			2.0±0.01	**100**	**SA/SD**
											2.2±0.01	**20**	2.2±0.02	**25**	**SA-peptide**
											2.9±0.01	**3**			
		3.7±0.01		3.2±0.01	**25**	3.5±0.01	**25**	3.8±0.04	2.6±0.01	**4**	3.7±0.03	**25**	3.3±0.01	**25**	**GNBP1**
				4.0±0.3	**50**	4.5±0.2	**10**		3.6±0.01	**25**	4.8±0.06	**10**	4.3±0.01	**75**	**SA/SD-GNBP1**
		5.5±0.5		5.6±0.7	**5**				5.5±0.01	**1**	6.2±0.02	**3**	5.7±0.03	**3**	**GNBP1 dimer?**
			6.2±0.3										6.2±0.01	**3**	
						6.7±0.02	**1**						6.7±0.01	**3**	
								7.1±1.1			7.7±0.06	**1**	7.8±0.01	**10**	**SA-GNBP1-SD**
								11.4±0.4					8.9±0.01	**3**	
								12.8±0.3							
								24.3±0.2							
								35.7±0.5							
								38.1±0.9							

We show the sedimenting species observed in each mixture, as defined above, and where relevant their weight ratios calculated from the area under the g(s) curve. We have colored selected rows to indicate related species in multiple experiments and in the final column indicate our identification of some of the species.